Morphologies of poly(dimethylsiloxane)–nylon-6 diblock copolymers and blends

C. A. Veith† and R. E. Cohen*
Department of Chemical Engineering, Massachusetts Institute of Technology, Cambridge, MA 02139, USA

and A. S. Argon
Department of Mechanical Engineering, Massachusetts Institute of Technology, Cambridge, MA 02139, USA
(Received 2 April 1990; accepted 13 June 1990)

The morphologies of poly(dimethylsiloxane)–nylon-6 diblock copolymers and binary/ternary blends with PDMS and nylon-6 homopolymers have been revealed by transmission electron microscopy (TEM). The spherulitic morphologies of materials cast from solution in 2,2,2 trifluoroethanol have been compared to the spherical microphase-separated structures obtained by annealing above the melting point of nylon-6. Either the PDMS rubber block length or the nature of the casting solvent can be employed to shift control of the morphology between mechanisms of microphase separation and crystallization. As a result, 'path-dependent' morphologies have been observed for PDMS–nylon-6 diblock copolymers and blends and these are explained in a unified manner via a conceptual phase diagram.

(Keywords: poly(dimethylsiloxane)–nylon-6 diblock copolymers; morphology; TEM)

INTRODUCTION

Although there have been recent studies revealing the supramolecular morphology of nylon-6 homopolymer[1,2], there are comparatively few studies that have elucidated the structure of rubber–nylon-6 copolymers at the sub-micron level. Attempts to prepare satisfactory transmission electron microscopy specimens of rubber–polyamide copolymers are often unsuccessful because the compliance of the rubber and the inherent toughness and undesirable wetting characteristics of the polyamide made microtoming (even cryo-ultramicrotoming) very difficult. Thus, most investigators[3–5] of rubber–nylon-6 copolymers have examined the surface morphology of fractured samples using scanning electron microscopy. The materials used in these earlier studies were predominantly graft copolymers of nylon-6 and various ethylene–propylene or ethylene–propylene–diene rubbers. The rubber was seen as large ($>1\ \mu m$) particles with a broad size polydispersity. Little could be discerned about the role of microdomain formation in competition with crystallization in these graft copolymers (or blends).

Simpler and more controlled morphologies can be formed from block copolymers for which the microdomain size and type depend in a straightforward manner on the block length[6,7]. Thus, the competition between crystallization and microphase separation can be interpreted more clearly. Wondraczek and Kennedy[8] have used transmission electron microscopy (TEM) to reveal the crystalline texture of di- and triblock copolymers of poly(isobutylene)–nylon-6. However, since the PIB block molecular weights were only about $10\ kg\ mol^{-1}$ and because only low-to-intermediate magnifications were employed, very little information was obtained concerning the spatial juxtaposition of the rubber to the nylon-6. Only coarse, spherulitic crystal texture was observed with no resolution of the rubber domains.

The work presented here has successfully revealed the sub-micron morphology of a new poly(dimethylsiloxane)–nylon-6 diblock copolymer via transmission electron microscopy. We present the morphologies of two PDMS–nylon-6 diblock copolymers possessing different rubber block lengths and polydispersities. Because rubber block length[6,7] and casting solvent[9–11] strongly influence the morphology of amorphous diblock copolymers, we have examined the influence of these variables on our PDMS–nylon-6 diblocks. The diblock morphologies are compared with domain size predictions of thermodynamic theories[12–14] for amorphous diblock copolymers. Previous work from this laboratory[15] showed clearly that casting and/or annealing histories influence the morphology of semicrystalline–amorphous diblock copolymers. These earlier observations are reinforced in the work reported here.

Morphologies of binary and ternary blends of one of the diblocks with homopolymers of nylon-6 and PDMS demonstrate the emulsification capabilities of this semicrystalline–amorphous diblock copolymer analogous to findings for amorphous–amorphous diblocks[16–18]. The observed morphologies of the PDMS–nylon-6 diblocks are discussed in terms of a conceptual temperature–composition phase diagram which depicts microphase separation in competition with crystallization. Each of these two competing mechanisms can dominate and govern the morphology; their competition can be used

* To whom correspondence should be addressed
† Current address: Department of Chemistry, University of North Carolina, Chapel Hill, NC, 27599, USA

0032-3861/91/091545-10

to explain previous experimental findings[19–21] for certain lamellar semicrystalline–amorphous diblocks as well as the morphologies of the PDMS–nylon-6 diblocks and blends studied here.

EXPERIMENTAL

Films of about 500–1000 Å were solution cast from 2,2,2-trifluoroethanol (TFEtOH) directly onto copper TEM grids. Subsequent thermal treatments such as annealing and melt recrystallization were conducted with the grid samples. Slow and moderate cooling rates were used: the 'moderate' programme moved from the melt at ≈250°C to room temperature in about 35 min whereas the 'slow' cooling took about 80 min. All ternary compositions (i.e. copolymer blended with both homopolymers) experienced the 35 min cooling history. Additional heavy metal staining was not required; sufficient contrast for TEM was obtained with unmodified specimens. Phillips 300 EM and 400 EM microscopes were used at accelerating voltages of 100 kV or 120 kV, respectively.

The WAXS equipment was a Rigaku Rotaflex with a rotating anode which operated at 50 kV and 60 mA and produced CuKα radiation filtered electronically and with nickel film. Detector to sample distance was 185 mm with a powder sample goniometer; the scans were obtained with a 0.2 degree step programme with a collection time of 10 s per step.

Details of the synthesis of the copolymers and the molecular-level characterization of the diblock copolymers are reported in detail elsewhere[22] and summarized in *Table 1*. Differential scanning calorimetry was performed via a DSC 4 (Perkin Elmer) using 10°C min^{-1} scanning rates.

RESULTS

Copolymer (3/100) has been extensively studied in blends with homopolymers and in undiluted form; copolymer (15/44) has been evaluated only as pure material. The two homopolymers are nylon-6 of $\bar{M}_w = 39.2$ kg mol^{-1} and $\bar{M}_n = 21.7$ kg mol^{-1} (ref. 23) and poly(dimethylsiloxane) of peak molecular weight c. 1 kg mol^{-1}. Note that both homopolymers have molecular weights less than the corresponding blocks of copolymer (3/100).

Poly(dimethylsiloxane)–nylon-6 diblock copolymers

The two PDMS–nylon-6 copolymers exhibit very different morphologies depending on sample preparation and thermal history. The siloxane block length markedly affects the solubility of the copolymer in TFEtOH, a very good solvent for nylon-6 ($\chi_{AS} = 0.09$ (ref. 24)). Thus, diblocks with short siloxane block lengths crystallize from TFEtOH prior to microphase separation whereas block copolymers with longer siloxane sequences may undergo microphase separation before crystallization. In this section, the morphologies of the diblock copolymers (3/100) and (15/44) resulting from both solution casting and melt crystallization will be presented.

Copolymer (3/100)

Before discussing the morphology of this copolymer, some comments are needed to clarify its molecular architecture. Proton n.m.r. and size exclusion chromatography (SEC) experiments revealed an average siloxane block length of only 3 kg mol^{-1} and a polyamide-6 block length of c. 100 kg mol^{-1}. The SEC of this diblock is shown in *Figure 1*, curve 1; the polydispersity of the siloxane block is extremely large due to significant depolymerization (backbiting) and chain transfer of the siloxane during the anionic growth of the polyamide-6 block[22,25]. The molecular weight range of the siloxane block is estimated[22] to vary from oligomeric up to as large as 30 kg mol^{-1}, and this molecular polydispersity has important consequences in regard to morphology as demonstrated below.

The morphology of copolymer (3/100) as cast from TFEtOH and annealed at 100°C, *in vacuo* is shown in *Figures 2a* and *b*. A spherulitic or axialitic morphology is seen where the darker spheres of c. 0.1–0.2 μm in size are the siloxane-rich regions. The spherulites are 3–5 μm in diameter. The lamellae which can be seen in more detail at higher magnification in *Figure 2b*, emanate from the centre of the spherulites and run continuously without interruption (but with branching) all the way to the boundaries. They resemble the smooth, gently curving, gradual fanning outward 'ribbon' structures found in bulk nylon-6 spherulites by Galeski *et al.*[1].

Figures 2a and *2b* also show randomly distributed spherical domains which apparently separated from the polyamide-6 before crystallization occurred. These

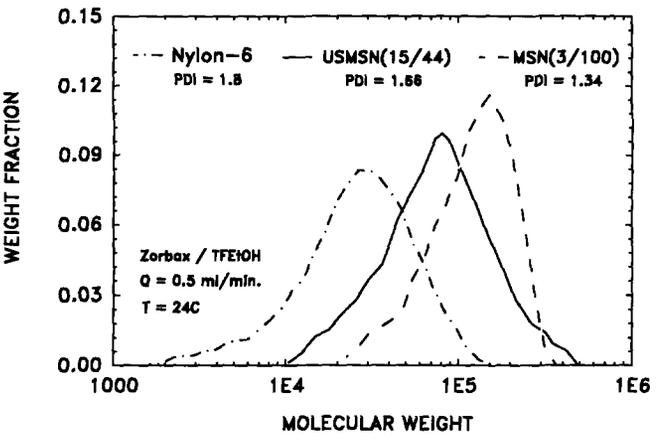

Figure 1 Size exclusion chromatograms of ---, (3/100) and ———, (15/44) diblocks plus –·–·–, allied nylon-6, as received for reference. PDI = polydispersity index

Table 1 Compositions of PDMS–nylon-6 diblock copolymers as determined from ^1H n.m.r. and SEC

Abbreviation	Polymer structure[a]	Number of repeat units			Composition (mol%/wt%)		
		PDMS	PMVS	PA6	PDMS	PMVS	PA6
(3/100)	PDMS–PMVS–PA6	40	10	885	4.3/2.9	1.1/0.8	94.6/96.3
(15/44)	PDMS–PA6	202	–	389	34.1/25.4	–/–	65.9/74.6

[a]Diblock (and triblock) copolymers containing PDMS = polydimethyl siloxane, PMVS = polymethylvinylsiloxane, PA6 = nylon-6

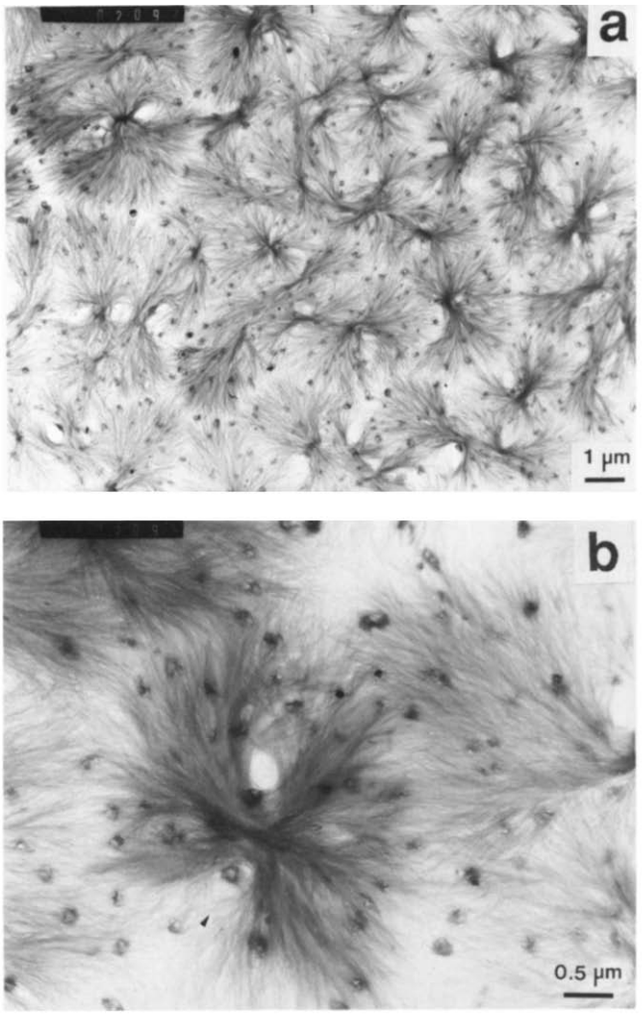

Figure 2 TEMs of (3/100) cast from TFEtOH and annealed at 100°C; (a) low magnification, (b) medium magnification. Arrows indicate wavy, zig-zag lamellae. Larger particles represent micellized PDMS prior to crystallization

microspherical domains arise from the immiscibility of the high molecular weight fraction of the siloxane blocks with the TFEtOH solvent. Hence for these PDMS-rich copolymer chains, microphase separation occurs prior to crystallization. When the spherulites are subsequently initiated, the chain-folded lamellae engulf the micro-domains of rubber to fill the volume.

Closer inspection of the 'rubbery-dotted' spherulites of *Figures 2* and *3* shows that the larger rubber particles are not completely featureless, i.e. some appear to be composite particles comprised of both nylon-6 and PDMS. This is shown in *Figures 3a* and *b*, as well as in *Figure 2b* where the particles seem to contain nylon-6 within them (e.g. the lighter regions of particle '2', *Figure 3b*). Also, some of the particles are actually aggregates of several smaller particles as seen throughout *Figures 2b* and *3a* (right side).

When the (3/100) copolymer is subsequently melt annealed, i.e. the cast film is heated above the melt temperature and cooled at a moderate rate, the morphology is altered dramatically. This result is shown in *Figure 4*. It is apparent that much of the siloxane has now pooled together into a micellar organization consisting of a siloxane core and a nylon-6 corona/matrix. The micrograph of *Figure 4* reveals different size particles ranging from c. 50 Å up to 500 Å, reflecting the breadth of molecular weight distribution of the siloxane block. Although no high temperature scattering experiments were done in the melt to ascertain its heterogeneous morphology, it is felt that the morphology of *Figure 4*

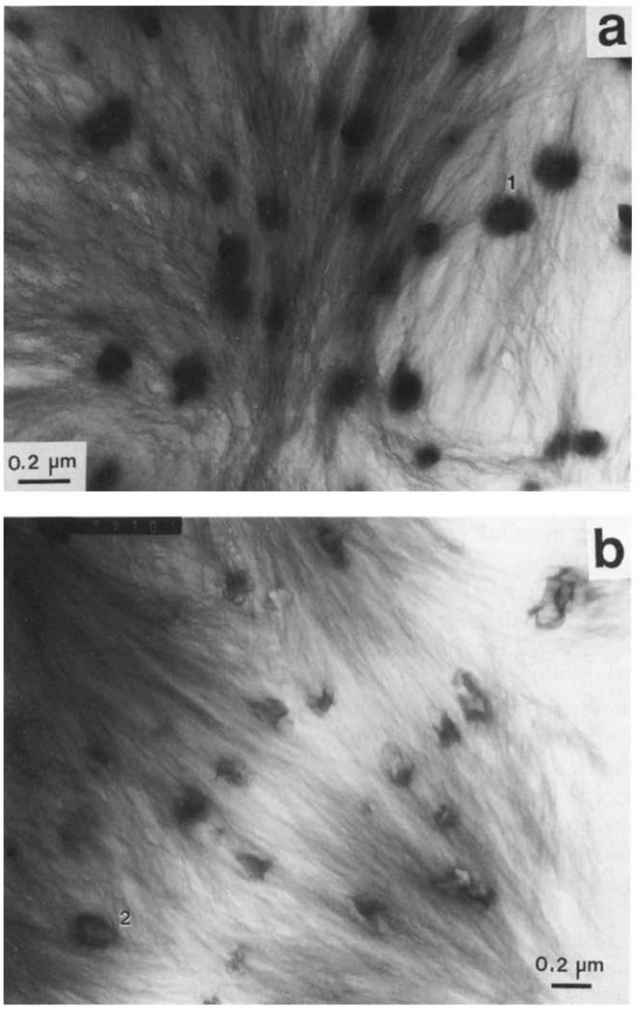

Figure 3 TEMs at high magnification of (3/100) cast from TFEtOH and annealed at 100°C. These micrographs show domain separation and aggregation of the siloxane particles within an axialitic sheath, panel a and within the interspherulitic region, panel b

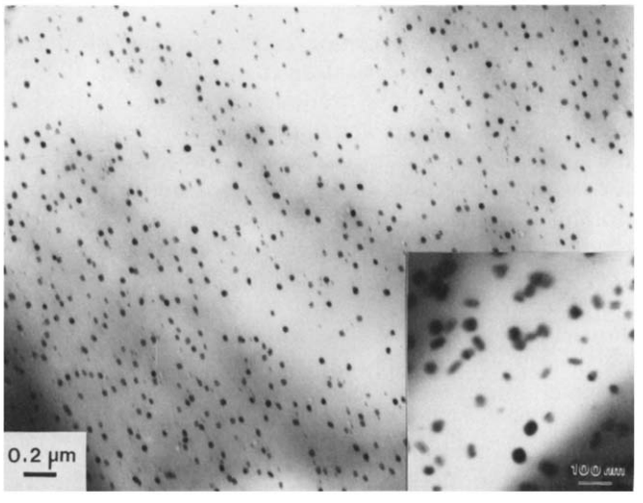

Figure 4 TEM of (3/100) melt annealed at 250°C and cooled at a moderate rate (45 min from 250 to 25°C). Insert shows higher magnification of a different region of the same sample

persisted in, and is fairly representative of, the amorphous melt state above the nylon-6 melting temperature. This is based on the strong incompatibility of PDMS ($\delta \approx 7.5$ (cal cm^{-3})$^{1/2}$) and nylon-6 ($\delta \approx 13$ (cal^{-3})$^{1/2}$). Although Leibler's theory[26] for microphase separation was derived for a weak segregation limit, use of his graphical results suggests that the temperature of the order–disorder transition of these PDMS–nylon-6 diblock copolymers should be well above their degradation temperature. Similar conclusions are obtained from application of the Helfand–Wasserman theory[12].

The crystallinity of the melt annealed (3/100) diblock is much lower than that of the same copolymer cast from solution. The enthalpy of fusion, ΔH_f, for the nylon-6 fraction of the solution cast material was about 28 cal g^{-1} *versus* 10 cal g^{-1} for the melt annealed diblock. Based on a purely α-form nylon-6 heat of fusion[27] of 45.4 cal g^{-1}, the crystallinity level of the nylon-6 fraction of the copolymer dropped from about 61 to 21% as a result of melt annealing.

Wide angle X-ray scattering data for copolymer (3/100) are shown in *Figure 5*, where curve 1 represents the film cast from TFEtOH solution and annealed at 180°C for 16 h *in vacuo*, and curve 2 is for the same material after it has been melt annealed and cooled (~40 min: 250 → 25°C). These data show the presence of primarily the α-form crystals in the solution cast material although the (200) reflection at 20.17° is suppressed in comparison to the (002) reflection at $2\theta = 24.00°$, a result which is seen to some extent in reaction injection moulded nylon-6 which crystallizes from its monomer during anionic polymerization (see curve 4 of *Figure 5*).

The melt annealed material possesses a much greater proportion of the γ-form crystals compared to the solution cast film. This is seen in *Figure 5*, curves 2 and 1, where the former possess 48% γ-form crystallinity *versus* only 9% γ-form in the solution cast sample. The fractions of the crystalline forms (α and γ) were calculated by a computer program[28], based on the work of Gurato *et al.*[29], which provides a least squares fit of five Gaussian peaks to the X-ray spectrum. Melt annealed copolymer (15/44), curve 3, shows a majority of the α-form. Also included in *Figure 5*, curve 5, is the spectrum for melt annealed Allied Capron nylon-6 for comparison.

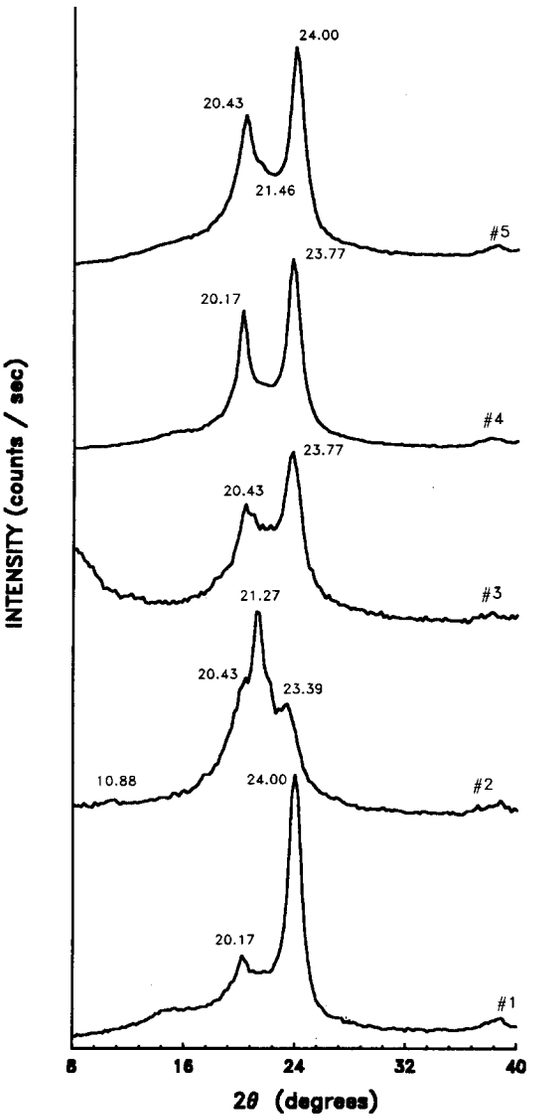

Figure 5 Wide angle X-ray scattering: curve 1, (3/100) solvent cast film from TFEtOH and annealed at 180°C, 91% α- and 9% γ-form; curve 2, (3/100) melt annealed at 250°C, 51.8% α- and 48.2% γ-form; curve 3, (15/44) melt annealed 250°C, 82.8% α- and 17.2% γ-form; curve 4, Monsanto RIM nylon-6, as received, 77.3% α- and 22.7% γ-form; and curve 5, Allied Capron nylon-6, melt annealed 250°C, 89.6% α- and 10.4% γ-form

Copolymer (15/44)

Molecular characterization of the polymer produced by ultrasonic copolymerization of ω-acyllactam–PDMS and ε-caprolactam has been described in detail elsewhere[22]. It has a narrower siloxane block polydispersity due to improvements in the catalyst and in the mixing during polymerization. Its PDMS block number-average molecular weight is 15 kg mol^{-1} with a nylon-6 block $\bar{M}_n$ of 44 kg mol^{-1}. The SEC chromatogram of copolymer (15/44) is shown in *Figure 1*, curve 2. The morphology of this copolymer as cast from TFEtOH is shown in *Figure 6a*. The spherical siloxane microdomains are clearly evident. The domains are about 250 Å in diameter and appear to be comprised completely of PDMS. This type of morphology suggests microdomain formation of the siloxane blocks prior to crystallization of the nylon-6 blocks. Although very long range order is not seen in the micrographs, some regions (see arrow) resemble a hexagonal structure.

The same material of *Figure 6a* was subsequently heated to 250°C for 10 min and cooled slowly from the melt: from 250°C to 220°C in 30 min followed by 0.2°C min^{-1} reduction until 180°C followed by subsequent cooling to 25°C in about 35 min. This thermal history resulted in the structure shown in *Figure 6b*. It appears identical to the unannealed solvent cast sample with similar domain size, siloxane sphere packing density and hints of long range order (arrows). Recall that this equivalency of melt annealed and solution cast morphologies for copolymer (15/44) is in sharp contrast to the difference in morphologies of (3/100) cast and subsequently melt annealed (*Figures 2, 3 versus Figure 4*). The (15/44) copolymer in either preparation method undergoes microphase separation before crystallization whether the siloxane blocks precipitate from the solvent or microphase separate in the melt of pure diblock. These observations indicate that the larger molecular weight amorphous PDMS blocks in a poor solvent (TFEtOH) microphase separate before crystallization, forcing the crystallization to occur in the interstitial regions around

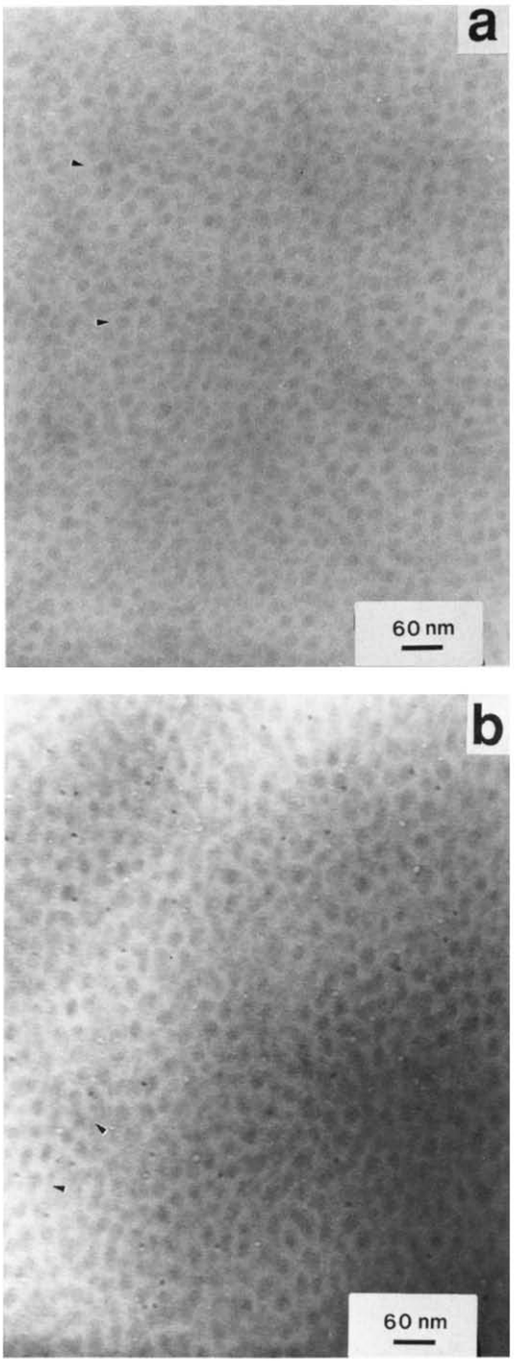

Figure 6 TEMs of (15/44) as (a) cast from TFEtOH solution and annealed at 100°C and (b) melt annealed at 250°C with an exceptionally slow cooling rate. Arrows indicate regions approaching a close-packed hexagonal structure

the preformed PDMS domains. This restriction of the semicrystalline blocks to the interstitial region does not necessarily translate into a decrease in crystallinity compared to the spherulitic (3/100) material or to lamellar chain-folded PEO–PI diblocks[19]. A very high density of nylon-6 ($\rho_{ny6} = 1.1949\ g\ cm^{-3}$; crystalline volume fraction, $\psi_C = 0.75$) was determined for copolymer (15/44) as cast from solution. Thus, the nylon-6 blocks are evidently able to crystallize with high efficiency in the interstitial regions between PDMS domains to generate such a high density.

To examine the effect of casting solvent on the morphology of the PDMS–nylon-6 diblock copolymer (15/44), we searched for a solvent more compatible with the amorphous PDMS block to delay phase separation while promoting crystallization. We used a 2:1 v/v mixture of toluene/TFEtOH which, at room temperature, dissolved the (15/44) diblock copolymer. The resulting morphology of an ultra-thin film cast from this solvent is shown in *Figure 7* where significant anisotropy of the film is seen. The domains are not perfect lamellae as found by Lotz *et al.*[20] or Gallot *et al.*[21,30–32] for PEO–polystyrene diblocks, but there is a substantial lamellar appearance quite different from the morphology of spherical domains obtained from pure TFEtOH. When the sample of *Figure 7* is heated to 250°C for 10 min and cooled rapidly at 20°C min^{-1}, the morphology (not shown) reverts back to a spherical microstructure essentially identical to that shown in *Figure 6b*.

Wide angle X-ray scattering of the melt annealed copolymer (15/44) is shown in *Figure 5*, curve 3. Predominantly α-form crystals are present in this material, again with the (002) peak at 23.78° being more prominent than the (200) reflection at 20.43° although only slightly. The amount of γ-form crystallinity calculated via peak deconvolution was 17.2%.

Binary blend of nylon-6 and copolymer (3/100)

One binary blend consisting of 43 wt% (3/100) and 57 wt% Allied hydrolytic nylon-6 was studied. This blend cast from TFEtOH gave a mixed morphology reflecting the fact that the nylon-6 homopolymer formed spherulites of its own as well as co-crystallizing with diblock chains within a growing spherulite. Consequently spherulites with and without spherical siloxane particles were formed; that is, the morphology of *Figures 2* and *3* was diluted with spherulitic homopolyamide-6.

The spherulitic morphology of the cast binary blend is shown in *Figure 8a* and at higher magnification in *Figure 8b*. Contrast enhancement has been achieved with phosphotungstic acid solution and OsO_4 vapour staining[1]. In *Figure 8a*, the amorphous regions are stained dark due to penetration of both staining agents leaving the crystalline regions relatively unstained and lighter in

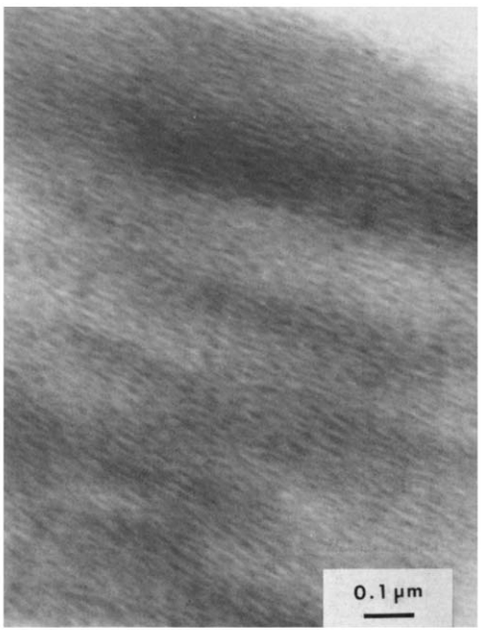

Figure 7 TEM of (15/44) as cast from a 2:1 Toluene:TFEtOH v/v solution, annealed at 100°C, *in vacuo*

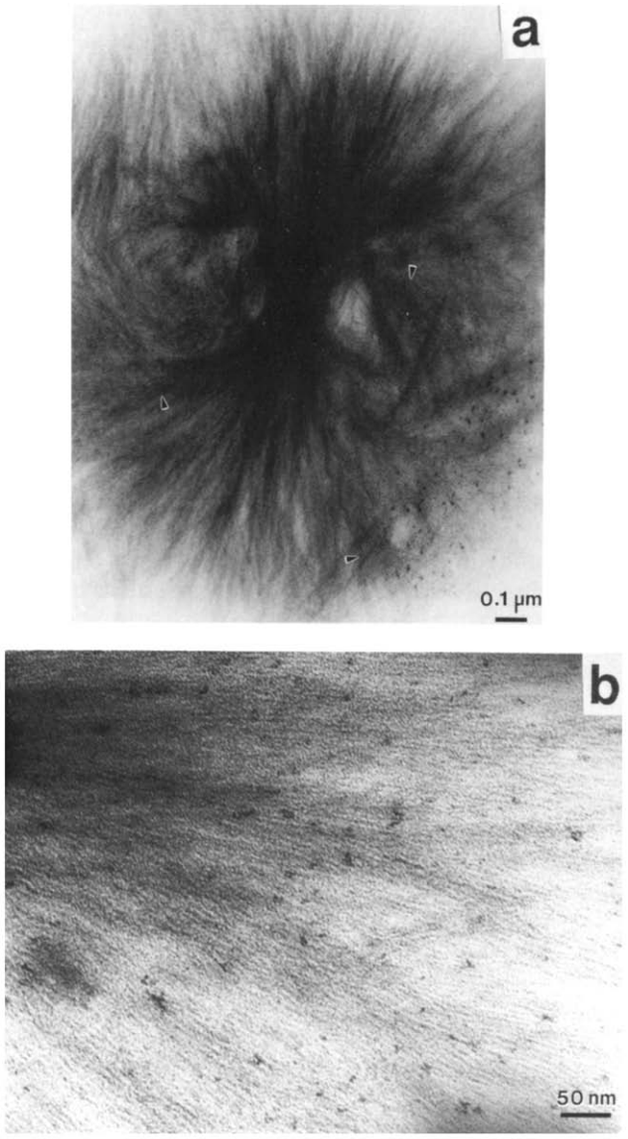

Figure 8 (a) TEM of spherulite from blend (43/57 wt%) (3/100) and nylon-6 homopolymer ($\bar{M}_n = 21.7\,kg\,mol^{-1}$) cast from solution and annealed at 100°C, *in vacuo*. Sample was stained with 1% aq. OsO_4 and 2% aq. PTA/BzOH solution (1:1 PTA:BzOH). Arrows indicate some discernible lamellar splay points. (b) TEM of same sample at higher magnification showing detail of lamellar structure

contrast except at the spherulite centres which are over-stained. The radiating lamellae can be seen emanating from the spherulitic centre, fanning outward and undergoing splaying (arrows)[33,34]. From *Figure 8a,b* we estimate that lamellae are on the order of 1 μm long and approximately 50 to 60 Å thick assuming that the lamellae are being viewed edge-on.

The axialite structure of *Figure 8a* does not possess the true spherical symmetry of a spherulite. The double circle or leaf-like structure has been observed in TEM replicas of isotactic polypropylene[35] and isotactic polystyrene[36]. The very small, dark, circular regions in the lower right corner of *Figure 8a* are the higher molecular weight rubbery blocks of the copolymer in this binary blend aggregated into micelles. While it can be surmised that the homopolyamide-6 chains of the diblock/homopolymer blend are completely intermixed with the diblock chains in solution, the kinetic nature of the crystallization process effectively partitions the components, preferring homopolyamide-6 and/or diblock chains with very short siloxane blocks for crystallization while enriching the remaining regime solution with copolymer molecules containing longer siloxane blocks.

Higher magnification of the 43/57 binary blend is depicted in *Figure 8b* which shows the lamellae to be c. 50–60 Å thick with the stained, amorphous interlamellar regions clearly visible in contrast to the white crystallites. Other darker regions within the radial lamellae represent short-to-moderate length siloxane blocks of copolymer (3/100) that participated in the lamellar growth. The lamellae resemble long, flat ribbons and continuously span large distances similar to TEM observations on ultra-thin sections of bulk nylon-6[1].

Melt annealing of the binary blend material gave a microstructure (not shown) very similar to that of *Figure 3*, i.e. spherical micelles of rubber dispersed in a nylon-6 matrix. Because of the large polydispersity of the rubber particle sizes and interparticle distances, it was impossible to quantitatively ascertain how the mean interparticle distance had changed with the addition of the homopolyamide-6. Small angle X-ray scattering (curve not shown) on melt annealed (3/100) copolymer revealed an intensity which decreased monotonically as a function of scattering vector which, according to Hosemann[37], will occur if the polydispersity of the system is greater than the packing density. Similar results have been seen by Martuscelli *et al.*[38] for graft copolymers of nylon-6 and EPR which are also known to be very polydisperse. Thus, an unambiguous comparison of the mean interparticle distances for the melt annealed copolymer and the binary blend could not be obtained.

Ternary blend

A ternary blend composition was explored to examine the ability of the copolymer to emulsify nylon-6 and homopoly(dimethylsiloxane) blends. The blend is denoted as 38/51/11 blend, where the numbers represent the weight percent of each of the three components: block copolymer (3/100), Allied nylon-6, and $1\,kg\,mol^{-1}$ PDMS. Both solution cast and melt annealed samples were examined in TEM.

The solution cast morphology of the 38/51/11 ternary blend (containing 12 wt% total rubber) is shown in *Figure 9*; the 1–3 μm diameter spherulites are readily seen. This morphology looks like a logical extension of

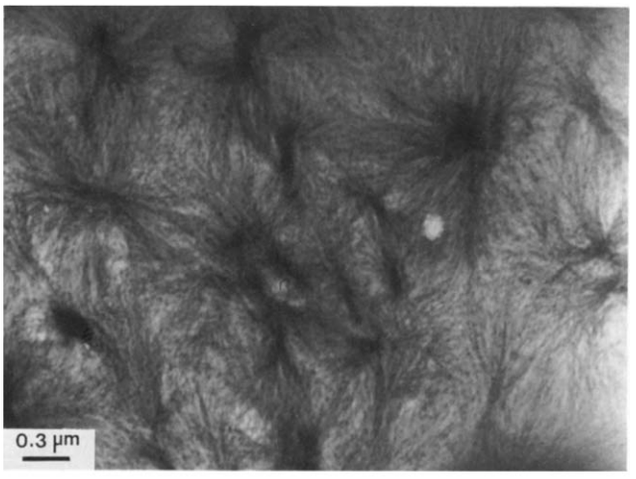

Figure 9 TEM of ternary blend (3/100)/nylon-6/PDMS 38/51/11 wt% as cast from solution, annealed 100°C

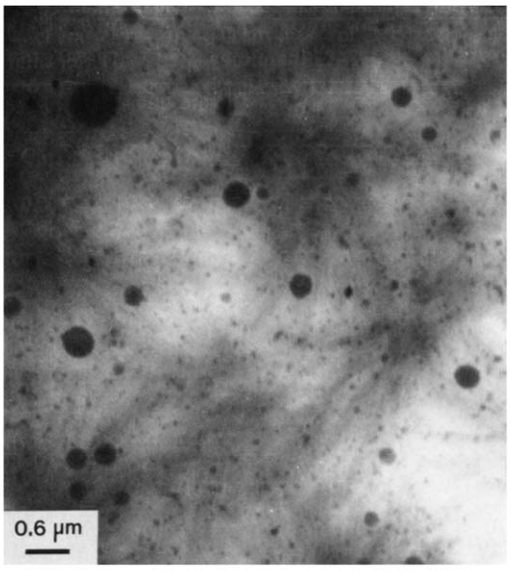

Figure 10 TEM of ternary blend (3/100)/nylon-6/PDMS 38/51/11 wt% after melt annealing the cast film

the (3/100) copolymer morphology shown in *Figures 2* and *3* with approximately spherical domains of siloxane (from both diblock and homopolymer) randomly distributed throughout the lamellar sheaths of the spherulites, but now at greater concentration. This unusual morphology has a significant amount of free rubber emulsified into small, well dispersed domains within a spherulitic superstructure. Differential scanning calorimetry measurements showed an exceptionally large (84%) crystallinity for the 38/51/11 ternary blend compared to 60% for the (3/100) copolymer. The melt annealed ternary blend 38/51/11 (*Figure 10*) shows spherulites ranging from 2–6 μm in diameter. The PDMS is dispersed throughout the spherulites in domains with a broad size distribution (500 Å–0.5 μm).

DISCUSSION

Comparison of semicrystalline–amorphous diblock morphologies

As detailed in *Table 2*, many earlier morphologies of semicrystalline–amorphous diblocks were found to be lamellar but in most cases the morphology was formed as the result of casting from a solvent preferential to the amorphous block. *Table 2* correlates the observed microstructures in the literature with the experimental/compositional parameters for solution cast block copolymers containing a semicrystalline block. Solvents which are preferential to the amorphous block can lead to non-equilibrium microdomain morphologies because the crystallizable block can precipitate from solution and crystallize, forcing the amorphous domains to adopt non-equilibrium conformations in bulk. This hypothesis is borne out by the data in *Table 2* where the PEO–PI diblocks of Hirata *et al.*[19] are seen to transform from spheres to cylinders to lamellae depending on diblock composition when cast from a non-selective solvent (benzene), in which microphase separation controls the morphology. When these same copolymers are cast from ethylbenzene, a selective solvent for the PI block, then only lamellar crystal morphologies are seen. The choice of a good solvent for the semicrystalline block facilitates microphase separation followed by crystallization, thereby permitting the microdomain morphology to approach equilibrium prior to crystallization.

Similarly, the work of Gervais and Gallot (*Table 2*) shows that for copolymers cast from solvents which are preferential to the amorphous block at temperatures below the melting point, only a lamellar morphology is observed. But if these same copolymers are heated above the melting point, then transformation occurs from lamellar to hexagonal-packed cylinders for certain asymmetric compositions. These examples, along with the additional data of *Table 2*, indicate that the preferred morphology for a semicrystalline/amorphous block copolymer is not necessarily lamellar, but depends, as is the case for wholly amorphous diblock copolymers, on the composition. As a consequence, some of the lamellar microstructures detailed in *Table 2* would prefer to be cylindrical or spherical but they are 'locked' into the lamellar structure when cast from solution due to crystallization control of the morphology. For diblocks with compositions near 50/50, the lamellar morphology will be formed regardless of casting conditions and can be annealed at sufficiently high temperatures to approach an equilibrium morphology.

Conceptual phase diagram for PDMS–nylon-6 diblock copolymers: path-dependent morphologies

The solution cast samples were all highly crystalline and, except for copolymer (15/44), they were spherulitic. Taken overall, the observed morphologies suggest a competition between microphase separation and crystallization phenomena which is controlled by a number of parameters including the block lengths, casting solvent and temperature. For the (3/100) diblock copolymer with its very polydisperse siloxane block lengths, both crystallization and microphase separation can occur simultaneously during solution casting. When this copolymer is cast from solution in TFEtOH, a good solvent for nylon-6, the chains with the high molecular weight siloxane blocks micellize before any crystallization has taken place. The location of this micellar transition of the long siloxane blocks from homogeneous solution (H) to a microphase separated structure (M) is represented in *Figure 11* by the curve designated CMC and 2, where the 2 represents the higher molecular weight fraction of the siloxane blocks in the copolymer. This shape and location of this boundary is shown schematically by the dashed lines in *Figure 11*.

In addition to the CMC, a description of the crystal–liquidus (c–l) curve is required to understand the competing process of crystallization from solution. A conventional melting point depression equation can be used to calculate a crystal–liquidus curve for nylon in TFEtOH. Curve c–l in *Figure 11* was determined using $\chi_{AS} = 0.09$[24].

In the casting process used in this work, the CMC transition occurs at a given composition of polymer as solvent is continuously removed (i.e. moving left to right along the dashed line abcde in *Figure 11*). For the fraction of the broad molecular weight distribution containing the longer siloxane blocks (CMC curve 2), the CMC (at point b) is achieved before the crystal–liquidus (c–l) curve is reached at c; therefore, microphase separation precedes crystallization. This is the event which produces the spherical microdomains of PDMS seen in *Figures 2, 3* and *6a*. For diblock (15/44), all of the siloxane blocks

Table 2 Summary of experimental conditions and morphologies of solvent cast semicrystalline–amorphous diblock copolymers

Author(s)	Ref.	T (°C)	Blocks[a]	Composition (wt%)	Solvent[b]	Morphology
Lotz *et al.*	20	25	EO–Sty	72–28	EtBz	lamellar
			EO–Sty	60–40	EtBz	lamellar
			EO–Sty	34–66	EtBz	lamellar
			EO–Sty	32–68	EtBz	lamellar
Hirata and Kawaii *et al.*	19	30	EO–I	76–24	Bz	Is spheres
			EO–I	72–28	Bz	Is pseudo-rods
			EO–I	60–40	Bz	lamellar-like
			EO–I	23–77	Bz	EO spheres
			EO–I	76–24	EtBz	lamellar-hedrite
			EO–I	23–77	EtBz	lamellae
Skoulious	39	20	EO–Sty–EO	23–56–23	BuPhth	lamellae
Gervais and Gallot	21	25	EO–Sty	70–30	DEPhth	lamellae
			EO–Sty	70–30	Xyl	lamellae
			CL–Sty	65–35	DEPhth	lamellae
	30	<50	EO–Sty	71–29	DEPhth	lamellae
			EO–Sty	48–52	DEPhth	lamellae
			EO–Sty	32–68	DEPhth	lamellae
		>65	EO–Sty	71–29	DEPhth	Sty hcp cyl
		(melt)	EO–Sty	48–52	DEPhth	lamellar
			EO–Sty	32–68	DEPhth	EO hcp cyl
	31	<45	EO–Bd	59–41	Xyl	lamellae
			EO–Bd	59–41	HOAc	lamellae
Kawaii *et al.*	40	20–40	EO–αMS	64–36	EtBz	lamellae
Cohen *et al.*	15	65	EB–Sty	11–89	Xyl	indeterminate
		125	EB–Sty	11–89	Xyl	EB spheres
Veith, Argon and Cohen	This	25	NY6–PDMS	75–25	TFEtOH	PDMS spheres
	paper		NY6–PDMS	75–25	TFEtOH/Tol	lamellar-like
			NY6–PDMS	95–5	TFEtOH	PDMS spheres/spherulites

[a]EO = ethylene oxide, Sty = styrene, I = isoprene; CL = caprolactone; Bd = butadiene, 90% 1,2 and 10% 1,4-*trans*; αMS = α-methylstyrene; EB = ethylene-co-1-butene

[b]EtBz = ethylbenzene (selective towards Sty block); Bz = benzene (approximately non-selective solvent); BuPhTh = butylphthalate (selective towards Sty); Xyl = xylene (non-selective-to-slightly selective towards Sty); HOAc = acetic acid (selective towards EO), DEPhth = diethyl phthalate (selective towards styrene); 1:2 v/v TFEtOH/toluene mixed solvent

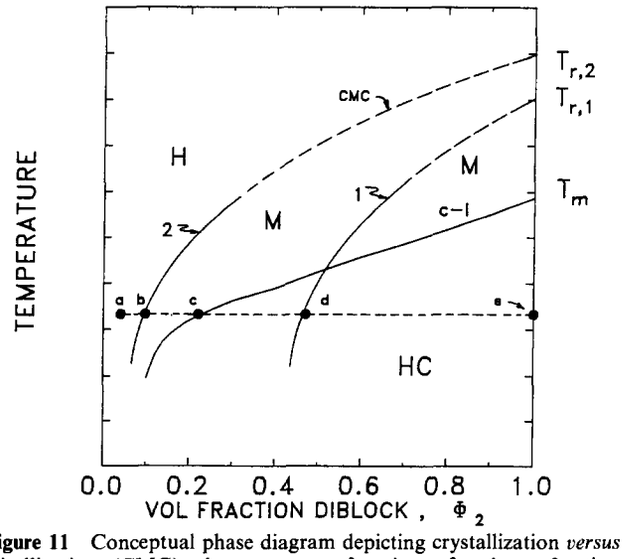

Figure 11 Conceptual phase diagram depicting crystallization *versus* micellization (CMC) phenomena as function of volume fraction diblock, Φ_2 and temperature; H = homogeneous fluid, M = mesophase, HC = crystalline solution; '2' = diblock with longer siloxane block length; '1' = diblock with shorter (more soluble) siloxane block length. Solvent TFEtOH, S, is preferential to nylon-6 block, A, $\chi_{AS} \doteq 0.09$

are long enough to micellize prior to crystallization whereas only the copolymers with the longer siloxane blocks of copolymer (3/100) micellize first.

For the lower molecular weight siloxane block fraction of copolymer (3/100), the CMC is shifted to higher copolymer volume fractions, as illustrated by the curve labelled 1. In this case the crystal–liquid binodal (at c) is reached prior to the corresponding CMC (at d). The copolymer becomes metastable in solution at point c and crystallizes before microdomain formation occurs. This point c in the casting process is responsible for initiating the spherulitic structure eventually seen in *Figures 2* and *3* for diblock (3/100). Crystallization proceeds until spherulite impingement fills the volume and engulfs the previously microphase separated blocks to give the morphology of *Figures 2* and *3*.

Alternatively, the occurrence of crystallization prior to microphase separation can be accomplished by using a solvent which is selective for the amorphous block. This is illustrated for the (15/44) diblock by the lamellar morphology observed in *Figure 7* when this copolymer was cast from a solvent mixture favourable to the siloxane block. In this case, crystallization preceded microphase

separation but not because of short PDMS block lengths, but rather because of preferential solvation of the amorphous block by the toluene-rich solvent. Also in this case, the CMC locus 2 is shifted to higher diblock concentration and is not reached in the practice of casting actual films because it lies under the c–l binodal. The morphology of *Figure 7* is not the stable equilibrium structure, and when the sample is melt annealed, it reorganizes into a lower free energy state identical to that shown in *Figure 6b*.

The melt annealing procedure can be viewed in terms of the transitions that occur for the pure copolymer at $\phi_2 = 1$ (right-hand ordinate in *Figure 11*). The first transition experienced upon heating the bulk copolymer is the melting of the crystallites which produces the stable mesophase structure of PDMS spheres in a melt of the nylon-6 block. The order–disorder transition temperatures, T_r, on the phase diagram may or may not actually exist for PDMS–nylon-6 diblocks at temperatures below their degradation limits. Continued heating would, in principle, transform the low molecular weight block copolymer from a structured mesophase to a homogeneous fluid at $T_{r,1}$ while the higher molecular weight material remains in the mesophase. Further heating finally converts all the high molecular weight copolymer into a single homogeneous fluid. Thus, as a result of the polydispersity, a range of microphase separation temperatures would be observed in principle for copolymer (3/100). As was mentioned previously, however, these T_r values almost certainly lie well above the degradation temperature due to the large incompatibility of the PDMS and nylon-6 blocks.

Morphology of PDMS–nylon-6 diblock copolymers and comparison with micelle theory

Because the PDMS and nylon-6 blocks are highly incompatible, the narrow interphase approximation (NIA) theories of Helfand[6,12] and Semenov[14] are applicable to describe the mesophases of our pure diblocks. Helfand's theory uses a mean-field statistical thermodynamic approach. Recently, Semenov has developed an analytical methodology to solve the equilibrium mesophase structure for highly incompatible blocks. The system passes from the disordered state to the ordered mesophase whose domain microstructure is determined solely by f, the fractional composition of the diblock, χ_{AB} and N, the total number of segments in the diblock.

Even though our copolymers crystallize from the melt, it is instructive to compare the observed microphase separated morphologies with predictions of these theories, assuming that the morphological dimensions seen at room temperature are not very different from those of the heterogeneous melt which exists above T_m (but below T_r). Using a value of $\chi_{AB} = 4.3$ (estimated from solubility parameter data), Semenov's model for a spherical mesophase gives the results shown in *Table 3*. Estimates from the TEM micrographs were used for this comparison. Due to its large polydispersity, a periodicity value could not be calculated for copolymer (3/100). The Semenov theory overpredicts the characteristic domain size for both copolymers, with better agreement for the (3/100) diblock which contains PDMS block lengths. Also shown in *Table 3* are the predictions from Helfand's theory for the equilibrium domain sizes of these diblocks. As seen in *Table 3*, the agreement between theory and experiment is reasonable. The success of both of these theories lends support to the hypothesis that the spherical, melt annealed morphology of both diblocks is close to equilibrium due to micellization control of the morphology. In addition, these calculations suggest that when the spherical, micellized morphology of copolymer (15/44) was formed from solution, it was close to an equilibrium morphology. This obviously is not the case for the solution cast films containing diblock (3/100) which are spherulitic due to crystallization control.

CONCLUSIONS

The morphologies of the PDMS–nylon-6 copolymers and of binary and ternary blends containing these copolymers show a variety of unusual features. For the solution cast copolymer (3/100), these features include interlamellar poly(dimethylsiloxane) and occluded spherical poly(dimethylsiloxane) microdomains within spherulites. Both copolymers when cast from solution show evidence of competition between microphase separation and crystallization. When these cast samples are melt annealed, both diblock copolymers possess a spherical mesophase of PDMS in a nylon-6 matrix although with different packing densities. Both binary and ternary blends show evidence of the spherulitic structure in solution cast and melt annealed samples.

The facts that the morphology of copolymer (15/44) does not change upon annealing and that the physical dimensions agree well with theoretical predictions suggest that this morphology is close to equilibrium. However, when this same diblock is cast from a solvent preferential to the amorphous block, the PDMS morphology is no longer spherical but instead approaches a lamellar microstructure similar to morphologies observed earlier for semicrystalline–amorphous diblocks. During annealing, this morphology attempts to rearrange itself towards the spherical microdomain structure.

The axialitic morphology of copolymer (3/100) when cast from solution has been explained in terms of a conceptual phase diagram which illustrates the competition between microphase-separation and crystallization.

Table 3 Comparison of theory with observed mesophase structure for PDMS–nylon-6 diblock copolymers

	(15/44)			(3/100)		
Physical property[a]	Semenov[13]	Helfand[12]	Expt	Semenov[13]	Helfand[12]	Expt
Spherical domain diameter (Å)	490	247	250	170	83	150–500
Periodicity (Å)	565	345	300–400	390	237	[b]

[a]Samples prepared via melt annealing
[b]Too polydisperse to calculate a periodicity

These competing mechanisms help to explain the variations in microstructure of solution cast semicrystalline–amorphous diblocks discussed in the literature. For our diblocks in TFEtOH, higher molecular weight siloxane blocks undergo micellization before crystallization; the attached nylon-6 blocks subsequently crystallize. For diblock chains with short siloxane blocks, crystallization precedes micellization and the material becomes locked into a non-equilibrium morphology. This non-equilibrium constraint is released when the material is annealed above the nylon-6 melting point and this permits restructuring and reorganization of the PDMS into spherical microdomains.

The emulsification ability of the (3/100) copolymer has been demonstrated in the binary and ternary blends with one or both homopolymers. This behaviour is seen whether the material is cast from solution or melt recrystallized. The solution cast samples are much more crystalline than the melt annealed counterparts.

ACKNOWLEDGEMENTS

This research has been supported by the National Science Foundation via the MIT Center for Materials Science and Engineering under Grant DMR 87-19217.

REFERENCES

1 Galeski, A., Argon, A. S. and Cohen, R. E. *Die. Makromol. Chem.* 1987, **188**, 1195
2 Schaper, A., Hirte, R., Ruscher, C., Hillebrand, R. and Walenta, E. *Coll. Polym. Sci.* 1986, **264**, 649
3 Borggreve, R. J. M., Gaymans, R. J., Schuijer, J. and Ingen Housz, J. F. *Polymer* 1987, **28**, 1489
4 Cimmino, S., D'Orazio, L., Greco, R., Maglio, G., Malinconico, M., Mancarella, M., Martuscelli, E., Palumbo, R. and Ragosta, G. *Polym. Eng. Sci.* 1984, **24**, 48
5 Greco, R., Lanzetta, N., Maglio, G., Malinconico, M., Martuscelli, E., Palumbo, R., Ragosta, G. and Scarinzi, G. *Polymer* 1986, **27**, 299
6 Helfand, E. and Wasserman, Z. R. in 'Developments in Block Copolymers' (Ed. I. Goodman), Applied Science, New York, 1982, Ch. 4
7 Meier, D. J. *Am. Chem. Soc., Polym. Prepr., Div. Polym. Chem.* 1982, **18**, 340, 837
8 Wondraczek, R. H. and Kennedy, J. P. *J. Polym. Sci., Polym. Chem. Edn* 1982, **20**, 173
9 Inoue, T., Soen, T., Hashimoto, T. and Kawaii, H. *J. Polym. Sci. A-2* 1969, **7**, 1283
10 Cohen, R. E. and Bates, F. S. *J. Polym. Sci., Polym. Phys. Edn* 1980, **18**, 2143
11 Bates, F. S., Berney, C. V. and Cohen, R. E. *Macromolecules* 1983, **16**, 1101
12 Helfand, E. and Wasserman, Z. R. *Macromolecules* 1978, **11**, 960
13 Semenov, A. N. *Macromolecules* 1989, **22**, 2849
14 Semenov, A. N. *Sov. Phys. JETP* 1985, **61**, 733
15 Cohen, R. E., Cheng, P. L., Douzinas, K., Kofinas, P. and Berney, C. V. *Macromolecules* 1990, **23**, 324
16 Molau, G. E. *J. Polym. Sci., Pt A* 1965, **3**, 1267, 4235
17 Riess, G., Kohler, J., Tournet, C. and Banderet, A. *Die. Makromol. Chem.* 1967, **101**, 58
18 Kohler, J., Riess, G. and Banderet, A. *Eur. Polym. J.* 1969, **4**, 173, 187
19 Hirata, E., Ijitsu, T., Soen, T., Hashimoto, T. and Kawaii, H. in 'Copolymers, Polyblends and Composites' (Ed. N. A. J. Platzer), Adv. in Chem. Series, American Chemical Society, Washington, DC, 1975, p. 288
20 Lotz, B., Kovacs, A. J., Bassett, G. A. and Keller, A. *Kolloid. Z. u. Z. Polym.* 1966, **209**, 97, 115
21 Gervais, M. and Gallot, B. *Polymer* 1981, **22**, 1129
22 Veith, C. A. *PhD Thesis*, Massachusetts Institute of Technology, 1989; Veith, C. A. and Cohen, R. E. *Makromol. Chemie* in press
23 Veith, C. A. and Cohen, R. E. *Polymer* 1989, **30**, 942
24 Mattiussi, A., Gechele, G. B. and Francesconi, R. *J. Polym. Sci. A-2* 1969, **7**, 411
25 Veith, C. A. and Cohen, R. E. *J. Polymer Sci., Polymer Chem.* 1989, **27**, 1241
26 Leibler, L. *Macromolecules* 1980, **13**, 1602
27 Liberti, F. N. and Wunderlich, B. *J. Polym. Sci. Pt A-2* 1968, **6**, 833
28 Galeski, A. Polish Academy of Sciences, Center for Molecular and Macromolecular Studies, Lodz, Poland, private communication
29 Gurato, G., Fichera, A., Grandi, F. Z., Zannetti, R. and Canal, P. *Die. Makromol. Chem.* 1974, **175**, 953
30 Gervais, M. and Gallot, B. *Die. Makromol. Chem.* 1973, **171**, 157
31 Gervais, M. and Gallot, B. *Die. Makromol. Chem.* 1977, **178**, 1577
32 Gervais, M. and Gallot, B. *Die. Makromol. Chem.* 1979, **180**, 2041
33 Bassett, D. C. and Olley, R. H. *Polymer* 1984, **25**, 935
34 Bassett, D. C., Mitsuhashi, S. and Keller, A. *J. Polym. Sci. Pt A* 1963, **1**, 73
35 Bassett, D. C. and Vaughn, A. S. *Polymer* 1985, **26**, 717
36 Norton, D. R. and Keller, A. *Polymer* 1985, **26**, 704
37 Hosemann, R. and Bagchi, S. N. 'Direct Analysis of Diffraction by Matter', North Holland, Amsterdam, 1962, Ch. 11
38 Martuscelli, E., Riva, F., Sellitti, C. and Silvestre, C. *Polymer* 1985, **26**, 270
39 Skoulious, A. E., Tsouladze, G. and Franta, E. *J. Polym. Sci., Polym. Symp., Pt C* 1963, **4**, 507
40 Kawaii, T., Shiozaki, S., Sonoda, S., Nakagawa, H., Matsumoto, T. and Maeda, H. *Die. Makromol. Chem.* 1969, **128**, 252